ChemComm

COMMUNICATION

View Article Online
View Journal | View Issue

Cite this: *Chem. Commun.*, 2014, 50, 14440

Received 21st August 2014,
Accepted 26th September 2014

DOI: 10.1039/c4cc06561a

www.rsc.org/chemcomm

Enhanced catalytic performance of Mn_xO_y–Na_2WO_4/SiO_2 for the oxidative coupling of methane using an ordered mesoporous silica support†

M. Yildiz,[ab] Y. Aksu,[c] U. Simon,[d] K. Kailasam,[e] O. Goerke,[d] F. Rosowski,[f] R. Schomäcker,*[a] A. Thomas[e] and S. Arndt*[ag]

The oxidative coupling of methane is a highly promising reaction for its direct conversion. Silica supported Mn_xO_y–Na_2WO_4 is a suitable catalyst for this reaction. In this study, a variety of different SiO_2 materials have been tested as supports. Surprisingly, the application of ordered mesoporous silicas, here exemplarily shown for SBA-15 as support materials, greatly enhances the catalytic performance. The CH_4 conversion increased two fold and also the C_2 selectivity is strongly increased.

The proven reserves of natural gas have enormous potential as alternatives to the decreasing reserves of crude oil.[1] The main component of natural gas is CH_4, the most stable hydrocarbon. Its conversion into value added products, particularly its direct conversion, remains a difficult challenge.[2,3] One possible direct conversion is the oxidative coupling of methane (OCM), as shown in eqn (1).

$$CH_4 + O_2 \rightarrow C_2H_6 \text{ or } C_2H_4 + H_2O \quad (1)$$

Although, a large number of catalysts have been studied,[4] a breakthrough has not been achieved yet, especially because many catalysts deactivate due to the harsh reaction conditions.[5,6] Mn_xO_y–Na_2WO_4/SiO_2 is a very active, selective and stable catalyst, a fact which has been confirmed by several research groups.[7–9] The current knowledge of this catalyst has recently been reviewed.[7] Moreover, a fluidized bed processing procedure was developed for the large scale preparation of this material[10] allowing its application in the OCM mini-plant at the Technische Universität Berlin.[11]

To optimize the catalytic performance and to understand the structure–activity relationship, a variety of different support materials for Mn_xO_y–Na_2WO_4 are under investigation by our research groups.[12] However, it can be concluded that most support materials show inferior or just comparable performance to SiO_2 as supports. On the other hand we observed a remarkable influence on the catalytic performance when different types of silica supports were used.

In this communication, we want to report on the observation that the application of SBA-15 leads to a greatly enhanced catalytic performance in comparison with any other studied SiO_2 supports. SBA-15 is an ordered mesoporous silica[13] which is widely used as a catalyst support in fundamental research.[14] Indeed as very narrow pore size distributions and highly ordered cylindrical mesopores can be prepared in this material, SBA-15 has significant advantages to study the dispersion of the supported active phase.[15] On the other hand, so far SBA-15 has not found its way to industrial applications, probably because much cheaper porous silicas can be prepared by other approaches. Furthermore, the ordered cylindrical pore structures have been described to be detrimental in terms of transport of substrates in the material, thus might cause severe diffusion limitations.[16,17] Here, we show that the application of SBA-15 can largely enhance the catalytic performance of an OCM catalyst, compared to commercially available porous silica supports.

This is most surprising as the silica support completely loses its ordered mesoporous structure during the preparation of the catalyst.

The prepared catalysts are shown in Table 1. For the preparation of the Mn_xO_y–Na_2WO_4/SiO_2 catalysts, a standard wet impregnation procedure was used, as described in the literature.[7] The detailed synthetic protocols can be found in the ESI.† Catalytic tests were performed using a 6-fold parallel reactor set-up and 50 mg of the catalyst. Details of the experimental setup can be found in the ESI.†

The measured surface areas of the prepared catalysts showed a drastic reduction compared to the pure support material *cf.* Table 1, which is caused by the phase transformation from amorphous SiO_2 to α-cristobalite yielding complete collapse of the ordered mesoporous structure of SBA-15.[7] This transformation is also observed by

[a] *Technische Universität Berlin, Institut für Chemie, Straße des 17. Juni 124, 10623 Berlin, Germany. E-mail: schomaecker@tu-berlin.de*
[b] *Gebze Institute of Technology, Department of Chemistry, 41400 Gebze, Kocaeli, Turkey*
[c] *Akdeniz University, Faculty of Engineering, Department of Material Science and Engineering, Dumlupinar Bulvari, 07058 Antalya, Turkey*
[d] *Technische Universität Berlin, Institut für Werkstoffwissenschaften und -technologien, Fachgebiet Keramische Werkstoffe, Secretariat BA 3, Hardenbergstraße 40, 10623 Berlin, Germany*
[e] *Technische Universität Berlin, Department of Chemistry, Functional Materials, Hardenbergstraße 40, 10623 Berlin, Germany*
[f] *UniCat BASF JointLab, Fakultät II, Secretariat BEL6, Marchstr. 6, 10587 Berlin, Germany*
[g] *PCK Raffinerie GmbH, Passower Chaussee 111, 16303 Schwedt/Oder, Germany*
† Electronic supplementary information (ESI) available. See DOI: 10.1039/c4cc06561a

Table 1 The codes of Mn_xO_y–Na_2WO_4/SiO_2 catalysts, the origin of support materials and surface areas of the applied silica support materials and catalysts

Silica support material			Surface area of the catalyst (m^2 g^{-1})		
Catalyst code	Origin	Comment	Surface area (m^2 g^{-1})	Before reaction	After reaction
Cat-1	Synthesized	SBA-15	616.9	6.8	4.2
Cat-2	BASF	D 11-10	105.4	6.7	3.1
Cat-3	Sigma	Silica gel, grade 923	492.3	2.8	3.9

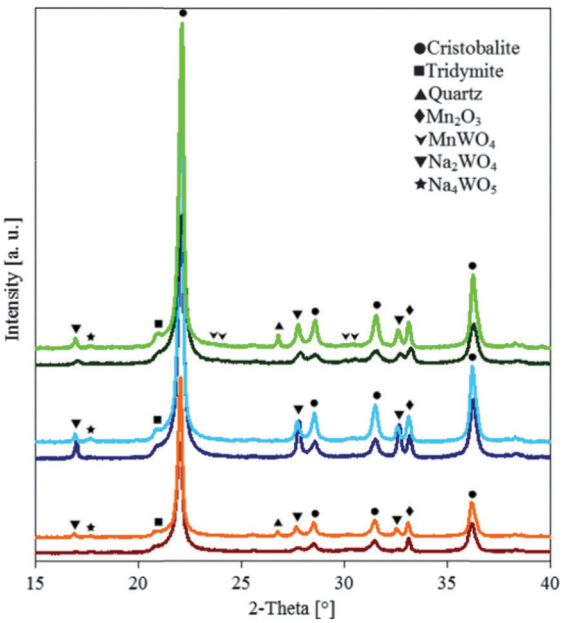

Fig. 1 XRD patterns of Cat-1 (green), Cat-2 (blue) and Cat-3 (red).

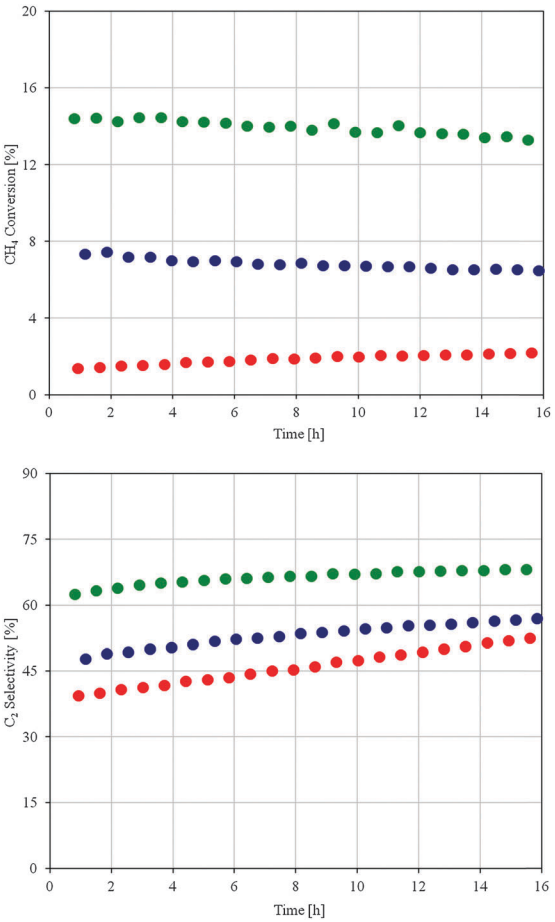

Fig. 2 CH_4 conversion as a function of time on stream (above) and C_2 selectivity as a function of time on stream (below) for Cat-1 (green), Cat-2 (blue) and Cat-3 (red) catalysts.

XRD measurements, as shown in Fig. 1. The loss of surface area during catalysis (before and after) is very small.

In Fig. 1, XRD patterns of the fresh and tested catalysts are represented in darker and lighter colors, respectively. In the fresh samples, α-cristobalite, tridymite, $MnWO_4$, Na_4WO_5 and Na_2WO_4 were detected. Moreover, Mn_2O_3 or braunite is found, but an unambiguous assignment was not possible due to the small number of signals and their low intensity. For all catalysts, α-cristobalite is formed as the main SiO_2 phase.

For the used samples of Cat-1 and Cat-3, quartz was additionally found. It is important to note that substantial differences in the phase compositions were not observed for all catalysts before and after the OCM reaction.

Elemental analysis furthermore revealed that the Mn, W and Na content on all silica supports is very similar (Table S2, ESI†). The three catalysts thus show very similar results regarding the surface area and composition and therefore no significant difference in their catalytic activity would be expected at this point.

The results of the catalytic tests are shown in Fig. 2. All tested catalysts exhibited a stable catalytic performance, with slightly increased selectivities.

Cat-3 was almost inactive for the oxidative coupling of methane under the applied reaction conditions, which is surprising, because its catalytic performance is even worse than most catalysts reported in the literature.[7] Cat-2 showed a comparable catalytic performance when compared to the other commercial SiO_2 support materials investigated in our laboratory (not shown). On the other hand, the performance of Cat-1 (SBA-15 supported) was outstanding with approximately 14% CH_4 conversion, *i.e.* it showed a two fold increase in conversion compared to Cat-2 with an even higher C_2 selectivity. As stated above, this significant increase in catalytic performance can be hardly explained by the surface area or composition of the three catalysts. However, BET, XRD and elemental analysis give no information on the distribution of active components on the catalysts.

In Fig. 3 and 4, SEM images and EDX mapping measurements are shown for the fresh catalyst Cat-1 and Cat-2. In Fig. 3, the rod shaped morphology of the SBA-15 support can still be seen in the SEM images of fresh Cat-1. The EDX mapping shows the homogeneous distribution of elements, especially tungsten. In contrast to this, for fresh Cat-2 irregular spherical silica particles can be seen with a more inhomogeneous distribution of elements, *cf.* Fig. 4. In addition, EDX-mapping of fresh catalyst Cat-1 showed even distribution of Mn with smaller particle sizes, while in Cat-2, Mn rich phases are observed as larger agglomerates on the silica support material.

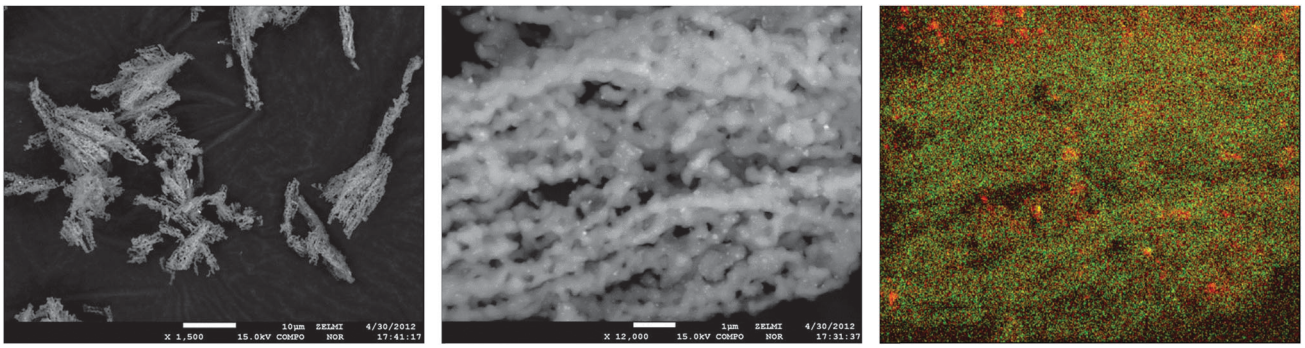

Fig. 3 SEM images of fresh Cat-1 (Mn_xO_y–Na_2WO_4/SBA-15) and EDX-mapping of W L-edge (green) and Mn K-edge (red).

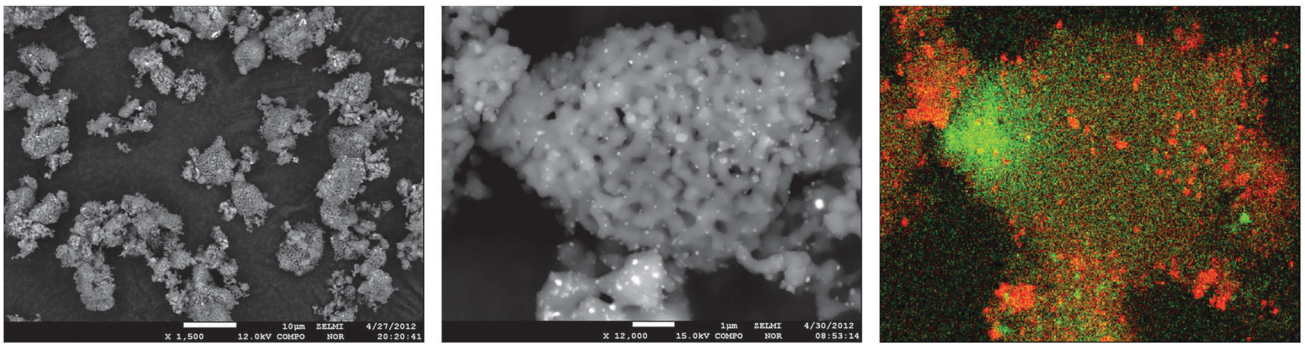

Fig. 4 SEM images of fresh Cat-2 (Mn_xO_y–Na_2WO_4/SiO_2) and EDX-mapping of W L-edge (green) and Mn K-edge (red).

For the first time in the research on the oxidative coupling of methane, one catalyst exists, which can be reproducibly prepared with good, medium, low and stable catalytic performances. The ongoing detailed studies will enable a first real view on the structure–activity relationship of this catalyst soon.

The catalytic performance of the Mn_xO_y–Na_2WO_4/SiO_2 catalyst is greatly enhanced by the application of SBA-15 as the silica precursor, approaching a level which might allow an industrial application. The explanation for this enhancement might be that the Mn_xO_y–Na_2WO_4 precursors are better dispersed in the small pores and the high surface area of SBA-15, which is reflected in the enhanced dispersion of the final catalyst even when the mesostructure of SBA-15 has collapsed after the thermal treatment. Optimization of this silica precursor, *e.g. via* adjusting the pore size and volume, could result in further improvement of the catalytic performance. Moreover, detailed structural characterization and comparison of these three catalysts, currently in progress, might give a first insight into the structure–activity relationship of this catalyst, a missing feature hindering the understanding of many catalytic systems, particularly for metal oxides. Unraveling such a kind of relationship could give room for further, perhaps even concerted, improvements.

This work is part of the Cluster of Excellence "Unifying Concepts in Catalysis" coordinated by the Technische Universität Berlin, supported by the Deutsche Forschungsgemeinschaft. Mr Yildiz is obliged to the Ministry of Education of the Republic of Turkey for financial support. We thank Dr Caren Goebel for electron microscopy measurements.

Notes and references

1 BP, BP Statistical Review of World Energy 2010, Online, 2010.
2 J. H. Lunsford, *Catal. Today*, 2000, **63**, 165.
3 A. Holmen, *Catal. Today*, 2009, **142**, 2.
4 A. M. Maitra, *Appl. Catal., A*, 1993, **104**, 11.
5 S. Arndt, G. Laugel, S. Levchenko, R. Horn, M. Baerns, M. Scheffer, R. Schlögl and R. Schomäcker, *Catal. Rev.: Sci. Eng.*, 2011, **53**, 424.
6 S. Arndt, U. Simon, S. Heitz, A. Berthold, B. Beck, O. Görke, J. D. Epping, T. Otremba, Y. Aksu, E. Irran, G. Laugel, M. Driess, H. Schubert and R. Schomäcker, *Top. Catal.*, 2011, **54**, 1266.
7 S. Arndt, T. Otremba, U. Simon, M. Yildiz, H. Schubert and R. Schomäcker, *Appl. Catal., A*, 2012, **425–426**, 53.
8 S. F. Ji, T. C. Xiao, S. B. Li, C. Z. Xu, R. L. Hou, K. S. Coleman and M. L. H. Green, *Appl. Catal., A*, 2002, **225**, 271.
9 S. B. Li, *J. Nat. Gas Chem.*, 2003, **12**, 1.
10 U. Simon, O. Görke, A. Berthold, S. Arndt, R. Schomäcker and H. Schubert, *Chem. Eng. J.*, 2011, **168**, 1352.
11 S. Stünkel, H. Trivedi, H. R. Godini, S. Jašo, N. Holst, S. Arndt, J. Steinbach and R. Schomäcker, *Chem. Ing. Tech.*, 2012, **84**, 1989.
12 M. Yildiz, U. Simon, T. Otremba, Y. Aksu, K. Kailasam, A. Thomas, R. Schomäcker and S. Arndt, *Catal. Today*, 2014, **228**, 5.
13 D. Y. Zhao, J. L. Feng, Q. S. Huo, N. Melosh, G. H. Fredrickson, B. F. Chmelka and G. D. Stucky, *Science*, 1998, **279**, 548.
14 (*a*) J. J. Zhu, X. Xie, S. A. C. Carabineiro, P. B. Tavares, J. L. Figueiredo, R. Schomäcker and A. Thomas, *Energy Environ. Sci.*, 2011, **4**, 2020; (*b*) G. Prieto, J. Zecevic, H. Friedrich, K. P. de Jong and P. E. de Jongh, *Nat. Mater.*, 2013, **12**, 34; (*c*) C. M. Yang, M. Kalwei, F. Schüth and K. J. Chao, *Appl. Catal., A*, 2003, **254**, 289; (*d*) P. Xiao, Y. Zhao, T. Wang, Y. Zhan, H. Wang, J. Li, A. Thomas and J. J. Zhu, *Chem. – Eur. J.*, 2014, **20**, 2872; (*e*) R. M. Rioux, H. Song, J. D. Hoefelmeyer, P. Yang and G. A. Somorjai, *J. Phys. Chem. B*, 2005, **109**, 2192.
15 P. Xiao, Y. Zhao, T. Wang, Y. Zhan, H. Wang, J. Li, A. Thomas and J. J. Zhu, *Chem. – Eur. J.*, 2014, **20**, 2872.
16 A. Zürner, J. Kirstein, M. Döblinger, C. Bräuchle and T. Bein, *Nature*, 2007, **450**, 705.
17 D. R. Rolison, *Science*, 2003, **299**, 1698.

